International Journal of ChemTech Research
CODEN (USA): IJCRGG ISSN: 0974-4290
Vol.7, No.3, pp 1377-1380, 2014-2015

ICONN 2015 [5th -7th Feb 2015]
International Conference on Nanoscience and Nanotechnology-2015
SRM University, Chennai, India

Electron Irradiation Effects on Structural Properties of Multiferroic $YMnO_3$

Prashanth K S Rao[1]*, Sheeja Krishnan[1], Manjunatha Pattabi[2], Ganesh Sanjeev[3]

[1]Department of Physics, Shree Devi Institute of Technology, Mangalore- 574 142, India
[2]Department of Materials Science, Mangalore university, Mangalagangotri- 574 199, India
[3]Microtron Centre, Mangalore university, Mangalagangotri - 574 199, India

Abstract : Multiferroic $YMnO_3$ nanoparticles have been synthesized by sol-gel method. The effect of 8 MeV electron irradiation on the structural properties of $YMnO_3$ nanoparticles under variable doses has been investigated. X-ray diffraction pattern confirms no phase change after irradiation. The crystallinity of the samples was found to improve with irradiation. However, microstrain developed in $YMnO_3$ nanoparticles due to electron irradiation causes peak broadening and shifting of X-ray diffraction pattern lines to lower diffraction angles. This indicates the presence of induced defects on irradiation. Various structural parameters under variable doses were calculated from XRD data.
Keywords: Electron Irradiation Effects, Structural Properties, Multiferroic $YMnO_3$.

Introduction

$YMnO_3$ (YMO) have been extensively studied for unique nature of multiferroism, which includes a spontaneous magnetization which can be switched by applied electric field and a spontaneous electric polarization which can be reoriented by applied magnetic field and a strong coupling of these two properties[1-5]. Multiferroic YMO nanoparticles can be synthesized by various techniques like sol-gel method[1,2], mechanochemical synthesis[3], modified pechini method[4], wet chemical synthesis[5] etc. YMO shows electric polarization along c axis due to buckling of MnO_5 layered accompanied by displacements of Y ions. Below the Neel temperature (T_N), the magnetic structure of YMO describes as frustrated antiferromagnetic (AFM) along the c-axis[2, 6]. Multiferroic YMO nanoparticles has potential industrial applications like nonvolatile ferroelectric random access memories, magentoelectric sensors, ferroelectric-gate-field-effect-transistors, transducer with magnetically modulated piezoelectricity, electric field controlled ferromagnetic resonance devices etc[4, 6]. YMO nanoparticles exhibit simultaneously ferroelectric order at 900 – 914 K (T_C)[2, 4] and antiferromagnetic transition at 70 - 77 K (T_N)[2, 6].

Irradiation on materials by high energy electron beam is a promising technique for modification of microstructure and physical properties of materials which have technological importance and scientific interest[6]. Electron irradiation on solid materials may create point defects or small defect associations[9]. High energy electron beam deposit their energy by columbic interactions on material, ionize the atoms and when the electron

beam has no sufficient energy to ionize the atoms, they can be trapped at the sites of defects which do pre-exist or created by the high energy electrons themselves. It is well know that material properties are mainly controlled by inherent defects or charge carriers, which are produced during irradiation. Interaction of energetic beam on material may form a variety of defect states and it depends on energy of the beam, fluency, temperature etc. Controlled introduction of defects in to a solid has been beneficially used to enhance its properties and consequently performance of devices based on them[7 - 10]. Thus, the present paper reports the modification in structural properties of YMO under 8 MeV electron irradiation.

Experimental:

For sol-gel method of synthesis of YMO nanoparticles, $Y(NO_3).6H_2O$ (purity of 99.8%, SIGMA-ALDRICH CO.), $Mn(CH_3COO)_2.4H_2O$ (purity of 99.5%, Merck Specialties Pvt Ltd) and ethylene glycol (purity of 99%, Merck Specialties Pvt Ltd) were used as starting material. $Y(NO_3).6H_2O$ and $Mn(CH_3COO)_2.4H_2O$ were dissolved in double distilled water to form an aqueous solution. An equal amount of ethylene glycol was added to the above solution and the solution was heated at 60 – 70^0C till a thick sol was formed. Constant stirring is done during the entire process. Sol was decomposed in an oven at 250^0C to get the dry fluffy material. The obtained precursor was calcined at 700^0C for 15 h in a furnace. Then the resulting calcined powder was reground and sintered at 1000 ^{0}C for 2 h in air.

The samples were irradiated with varying doses of high energy electrons of MeV range obtained from a variable energy Microton Accelerator at Mangalore University, Mangalore, India.

Rigaku D/max 2200PC X-ray diffractometer (XRD) with Cu Kα of wavelength 0.15418 nm was used for structural analysis at a scanning step of 2^0 min^{-1} in the range of $2\theta = 10^0$-100^0 before and after irradiation.

Results and discussion:

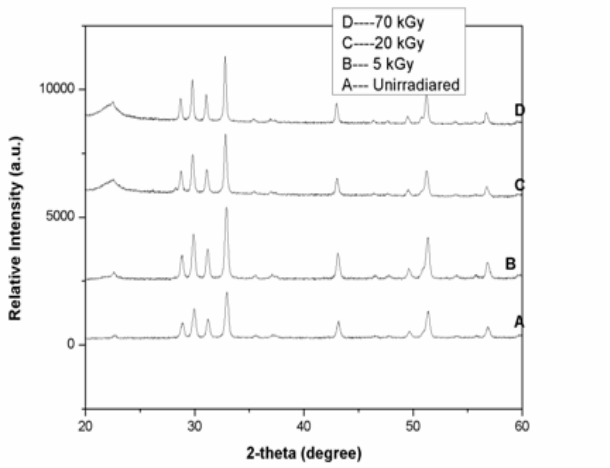

Fig. 1. XRD pattern of unirradiated and irradiated YMO Nanoparticles.

X-ray diffraction pattern of unirradiated and electron irradiated YMO samples at 5 kGy, 20 kGy and 70 kGy is shown in Fig. 1. Using the standard reference (JCPDS No. 25-1079), each peaks were examined and all the samples were found to exhibit hexagonal phase with space group $P6_3cm$. This suggests that all the samples are pure and do not show any phase change after irradiation. It was noticed that XRD peak intensities increase with increase in dose beyond 20 kGy, which indicates increase in crystallinity and good structural stability against electron irradiation. Increase in crystallinity due to deposition of electron irradiation energy on YMO samples can be explained on the basis of thermal spike model[11]. According to this model, due to the deposition of electronic energy on YMO samples, temperature increases along the track in a very short time interval. This induces crystallization in the material, which results in an increase in total amount of energy deposited into the lattice.

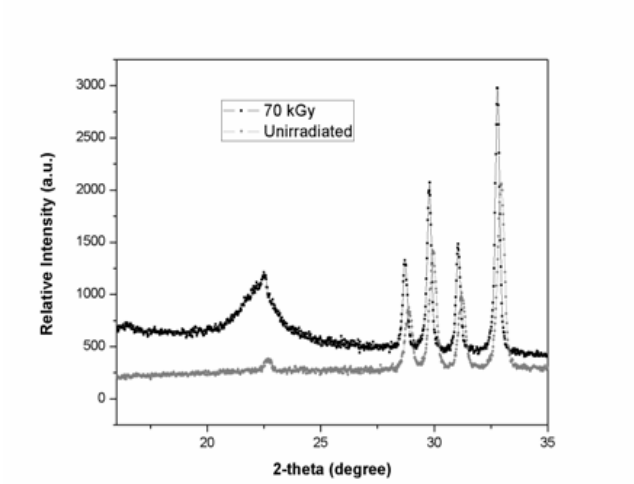

Fig. 2. XRD pattern of unirradiated and irradiated YMO nanoparticles.

It is evident from fig. 2 that, on irradiation the peak positions got shifted to a little lower diffraction angles due to changes in lattice spacing. This results in the development of microstrain and induced defects in the irradiated YMO samples[12, 13]. It was also observed from fig. 2 that, full width at half maxima (FWHM) values of irradiated sample is higher compared to unirradiated sample, which might be due to the presence of point/cluster defect in the irradiated YMO samples.

Table. 1. Various structural parameters of unirradiated and electron irradiated YMO nanoparticles at various doses.

Dose (kGy)	2-theta (deg)	FWHM (deg)	D (nm)	Microstrain (10^{-3})	Dislocation density ($10^{15}/m^2$)
unirradiated	22.72	0.3644	22	6.23	2.066
1	22.62	0.5645	14.8	9.65	4.565
5	22.53	0.5705	14.2	9.70	4.959
20	22.49	1.4927	5.43	25.39	33.91
50	22.48	1.3949	5.81	23.86	29.62
70	22.50	1.2287	6.06	21.01	27.23

Various structural parameters for unirradiated and electron irradiated samples have been calculated and listed in Table. 1. The average particle size (D) of unirradiated and irradiated samples was calculated using Scherrer's relation (1):

$$D = \frac{K\lambda}{\beta \cos\theta} \qquad \text{……. (1)}$$

where K is constant with a value of 0.89, λ the wavelength of X-ray (CuK_α radiation), β is FWHM value of diffraction peak, θ is the angle which the diffracted beam makes with the diffracting plane.

The average particle size of YMO samples were found to decrease after irradiation. High energy electron beam might push the atoms from their normal sites and split the molecules in to small fragments, which results in decrease in average particle size[6]. From Table. 1. it was also observed that average particle size increases and FWHM values decreases beyond 20 kGy . It may be due to induced coalescence of grain which results in rise in temperature of the samples. This also results in increase in crystallinity of the samples[14]. The microstrain and dislocation density can be calculated using relations (3) and (4)[11]:

$$\text{Microstrain} = \frac{\beta \cos\theta}{4} \qquad \text{…….(3)}$$

$$\text{Dislocation density} = \frac{1}{d^2} \qquad \text{……..(4)}$$

Microstrain and dislocation density increases on increasing electron dose. This indicates an increase in the amount of defects with radiation dose[12]. The strain developed during irradiation is mainly responsible for modification of different properties of the materials [9].

Conclusions:

X-ray diffraction shows that percentage of crystallinity of YMO nanoparticles increases with increasing electron irradiation doses. However, the crystallinity decreases for lower electron doses. The various structural parameters viz. microstrain and dislocation density were calculated from the data. Microstrain was found to develop in the grains of YMO nanoparticles due to electron irradiation. The X-ray diffraction data of irradiated YMO nanoparticles shows broadening and shifting of peaks.

References:

1. Kumar N., Gaur A. and Varma G. D., Enhanced magnetization and magnetoelectric coupling in hydrogen treated hexagonal $YMnO_3$, Journal of Alloys and Compounds, 2011, 509, 1060-1064.
2. Nelslc M. P., Stanojevic Z. M., Brakovic Z., Cotic P., Bernik S., Goes M. S., Marinkovic B. A., Varela J. A. and Brankovic G., Mechanochemical synthesis of yttrium manganite, Journal of Alloys and Compounds, 2013, 552, 451-456.
3. Zhang C., Su J., Wang X., Huang F., Zhang J., Liu Y., Zhang L., Min K., Zhijn W., Lu X., Yan F. and Zhu J., Study on magnetic and dielectric properties of $YMnO_3$ ceramics, Journal of Alloys and Compounds, 2011, 509,7738-7741.
4. Han T. C., Hsu W. L. and Lee W. D., Grain size-dependent magnetic and electric properties in nanosized $YMnO_3$ multiferroic ceramics, 2011,6,201.
5. Bergum K., Okamoto H., Fjellvag H., Grande T., Einarsrud M. A. and Selbach S. M., Synthesis, structure and magnetic properties of nanocrystalline $YMnO_3$,Dalton Transactions, 2011, 40, 7583.
6. Raneesh B., Saha A. and Kalarikkal N., Effect of gamma radiation on the structural, dielectric and magneto electric properties of nanostructured hexagonal $YMnO_3$, Radiation Physics and Chemistry, 2013, 89, 28-32.
7. Aparna S., Jali V. M., Sanjeev G., Parui J. and Krupanidhi S. B., Dielectric properties of electron irradiated $PbZrO_3$thin films, Bull. Mater. Sci., 2010,33 (2),191-196.
8. Sharma M., Kashyap S. C., Gupta H. C., Dimri M. C. and Asokan K., Enhancement of Curie temperature of barium hexaferrite by dense electronic excitations, AIP Advances, 2014, 4, 077129.
9. Bhat M., Kaur B., Kumar R., Joy P. A., Kulkarni S. D., Bamzai K. K., Kotru P. N. and Wanklyn B. M., Swift heavy ion irradiation effects on structural and magnetic characteristics of $RFeO_3$ (R = Er, Ho and Y) crystals, Nuclear Instruments and materials in Physics Research B, 2006, 243, 134-142.
10. Lee J., Chen C. L., Choi C. and Mori H., Electron irradiation induced phase change in nanomaterials, Proceedings of the Twenty-first (2011) International Offshore and polar Engineering Conference, Maul, Hawali, USA, June 19-24, 2011.
11. Vij A., Chawala A. K., Kumar R., Lochab S. P., Chandra R. and Singh N., Effect of 120 MeV Ag^{9+} ion beam irradiation on the structure and photoluminescence of SrS:Ce nanostructures, Physica B, 2010,405,2573-2576.
12. Mallick B., Behera R. C. and patel T., Analysis of microstress in neutron irradiated polyester fibre by X-ray diffraction technique, Bull. Matter. Sci., 2005, 28(6), 593-598.
13. Hassan H. E., Sharshar T., Hessien M. M. and Hemeda O. M., Effect of γ-rays irradiation on Mn-Ni ferrites: structure, magnetic properties and positron annihilation studies, Nuclear Instruments and Methods in Physics Research B, 2013, 304, 72-79.
14. Choudhury N., Singh F. and Sarma B. K., Effect of 100 MeV Ni8+ Ion irradiation on nanocrystalline PbS, Indian Journal of Pure & Applied Physics, 2012,50,325-328.

*****